Progress In Electromagnetics Research C, Vol. 68, 221–233, 2016

Two-Way Modified Wilkinson Power Divider for UWB Applications Using Two Sections of Unequal Electrical Lengths

Shaimaa A. Osman[1, *], Ayman M. El-Tager[2], Fawzy Ibrahim[3], and Ismael M. Hafez[4]

Abstract—This paper presents 2-way Power Divider (PD) for Ultra-Wideband (UWB) applications. The proposed power divider is realized using two cascaded sections of Wilkinson Power Divider (WPD) of equal characteristic impedances and unequal electrical lengths with inserted open stub to improve matching, isolation and to broaden the bandwidth. It is proved analytically using the "Even Odd Mode" analysis method and the ABCD matrix to obtain exact closed-form design equations. A detailed design methodology is introduced to facilitate the implementation without needing CAD optimization. To verify the proposed design methodology, a 2-way power divider is designed, fabricated on a Rogers RT/Duroid 5880 substrate and compared to other published 2-way microstrip power dividers. Measured data show good agreement with Electromagnetic (EM)-Circuit Co-Simulation, which proves the design equations and methodology. The proposed planar 2-way PD achieves an isolation ≥ 13.5 dB, input return loss ≥ 10 dB, output return loss ≥ 14.5 dB and exceeded insertion loss ≤ 0.9 dB (over the -3 dB splitting ratio) through the whole UWB range from 3.1 GHz to 10.6 GHz. Furthermore, it has a compact area of 22 mm $\times$ 15 mm, which provides 50% enhancement over similar microstrip PD circuits while achieving better isolation and matching.

1. INTRODUCTION

Power dividers and combiners are essential passive microwave components. Wilkinson Power Divider (WPD) [1] is the most practical and popular type as it provides matched ports, good isolation between output ports and lossless even when output ports are matched. In addition, equal division ratio WPD can be easily analyzed using "Even-Odd Mode" Analysis Method for three ports network by Cohn [2]. To overcome the narrowband problem of WPD, other structures are proposed for multi-band operation [3–5]. On the other hand, when designing an UWB WPD, three main criteria must be taken into consideration: isolation enhancement, matching improvement and bandwidth broadening.

Replacing the uniform quarter wavelength transmission line (TL) by tapered microstrip line as in [6–9] extends the bandwidth but on the expenses of large length, lots of passband ripples, and to have good S-parameters, two or three-section WPD is used. Another technique is to add a stub network to WPD to improve the bandwidth and the output return loss. Single stub is used as radial in [10], and as delta in [11], but both rely on EM simulators and optimizers. Double stubs are used in [12] and triple stubs used in [13], but it occupies large area and forces the designer to add DGS or other techniques to reduce the size. Microstrip to slotline transition is used in [14–16] to get UWB power divider with compact area, but it needs multilayer fabrication facility as well as full 3D EM simulation.

In [2], Cohn introduced an analytical solution to analyze an "N-Section" 2-way WPD containing N pairs of equal lengths TLs and unequal characteristic impedances as in Fig. 1. The circuit is analyzed using even-odd mode method to find the design formulas for the isolation resistors and the electrical

Received 21 July 2016, Accepted 7 September 2016, Scheduled 30 October 2016

* Corresponding author: Shaimaa Abdelaziz Mahmoud Osman (shaimaa.osman@yahoo.com).

[1] Telecommunication Engineering Department, Egyptian Russian University, Cairo, Egypt. [2] Electronics Engineering Department, MTC, Cairo, Egypt. [3] Misr International University, Cairo, Egypt. [4] Ain Shams University, Cairo, Egypt.

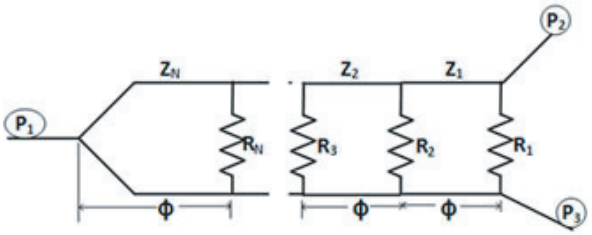

Figure 1. General circuit of the multiple-section three-port hybrid of [2].

length at which reflection coefficient is zero. The characteristic impedance values are decided from the desired fractional bandwidth ratio, and it relies on Young's Transformer Tables.

A broadband asymmetric multi-section WPD is proposed by Oraizi and Sharifi in [17] which is based on numerical optimization using method of least square. In [18], three sections of a non-uniform transmission line WPD are used to get broad bandwidth. Multiple-sections of WPD improve the isolation and broaden the bandwidth. It only needs to be implemented in a compact area. Therefore, this paper employs only two sections of WPD but with certain modifications to broaden the bandwidth and maintain compactness in the meanwhile. Matching improvement and bandwidth improvement can be achieved using open shunt stub matching network. In [19], Ahmed and Sebak introduced a single section Wilkinson Power Splitter (WPS) with adding a stub-matching network to broaden the bandwidth and also adding two transmission lines to the end of each branch to control the operating bandwidth. They stated the equations based on Cohn's procedure for their proposed design. To find the final formulas, they simplified the design by removing the output TLs without fixing them to Z_o which caused a huge difference between measurements and calculations.

Therefore, a novel design is proposed to overcome these problems as described throughout this paper. First, the design is based on a two-section WPD and a stub-matching network on each section to get broader bandwidth and improve the isolation, while fixing input and output ports to $Z_o = 50$ ohms to have perfect matching. Second, the two sections will have equal characteristic impedances in order to decrease ripples caused by discontinuities in widths. Third, change their electrical length to control the isolation and the matching bandwidths, while obtaining a compact design through the proper choice of electrical lengths ratio. Fourth, full analysis based on even-odd mode method and ABCD matrix is introduced to obtain exact closed-form expression and minimize the difference between the calculations and measurements.

In this paper, a UWB 2-way two-section WPD of unequal electrical lengths is proposed with single stub-matching network on each section. The proposed circuit is analyzed, designed and implemented based on the exact closed-form expressions. Section 2 introduces the structure of the proposed power divider. Section 3 explains the analytical solution for the proposed power divider. A parametric analysis for the electrical length ratio between sections one and two is reported in Section 4. The numerical solution of the 2-way power divider along with its simulation, implementation algorithm and comparison with other similar published 2-way power dividers is reported in Section 5. Finally, Section 6 concludes this paper.

2. STRUCTURE OF THE PROPOSED POWER DIVIDER

A schematic diagram of the proposed UWB 2-way power divider is shown in Fig. 2. The divider consists of two sections of modified WPD. The "*first section*" consists of primary transmission line (TL) of characteristic impedance Z_1, electrical length θ_1, an open shunt stub of characteristic impedance Z_{s1}, and electrical length θ_{s1}, in addition to secondary TL of characteristic impedance Z_1 and electrical length θ_{11}. The first section has an isolation resistor of R_1. Similarly, the "*second section*" has a primary TL of (Z_1, θ_2), stub matching network of (Z_{s2}, θ_{s2}) and secondary TL (Z_1, θ_{22}), and has a second isolation resistor of R_2. To achieve perfect matching, the input and output TLs are chosen to have characteristic impedance $Z_o = 50\,\Omega$.

The proposed structure shown in Fig. 2 is difficult to analyze, as the number of variables is big. Therefore, to analyze the circuit, we simply replaced every Tee-section with its equivalent transmission

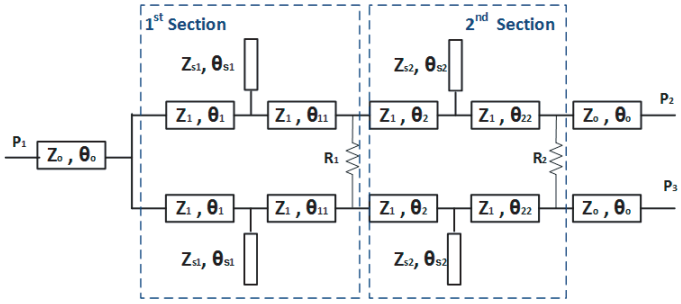

Figure 2. The schematic diagram of the proposed UWB 2-way power divider.

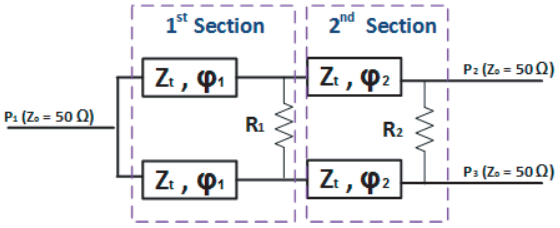

Figure 3. Simplified 2-way PD after fixing the input and output TL at Z_o and replacement.

line to get the simplified figure shown in Fig. 3, where the even-odd mode method can be applied as in Section 3.1. The relation between each TL and T-section is obtained using the ABCD matrix as in Section 3.2.

3. ANALYTICAL SOLUTION FOR THE PROPOSED PD

The analysis starts by replacing each section with its equivalent single transmission line as shown in Fig. 3. The novel idea of this paper is to examine the case of unequal electrical length transmission lines with equal characteristic impedances i.e., $\varphi_1 \neq \varphi_2$, $Z_{t1} = Z_{t2} = Z_t$.

3.1. Even-Odd Mode Analysis

The divider is symmetric as shown in Fig. 4; therefore, it can be analyzed using "even-odd mode" method as follows:

1. The voltage generators V_{g2} and V_{g3} are applied at the output ports.
2. The input impedance Z_o is divided into 2 parallel impedances, each of value 2 Z_o.
3. The isolation resistor R_1 is divided into 2 resistors, each of value $R_1/2$, and similarly R_2 is divided into 2 resistors, each of value $R_2/2$.
4. Two excitation modes are applied: Even mode and Odd mode.

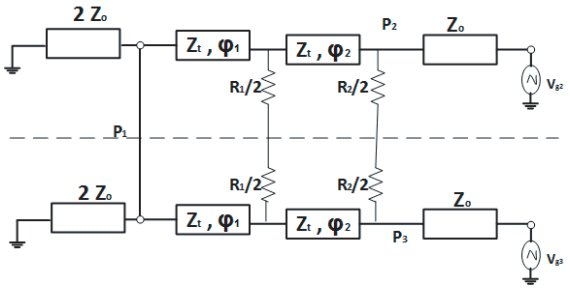

Figure 4. The proposed 2-way PD in symmetric form ready for even-odd mode analysis.

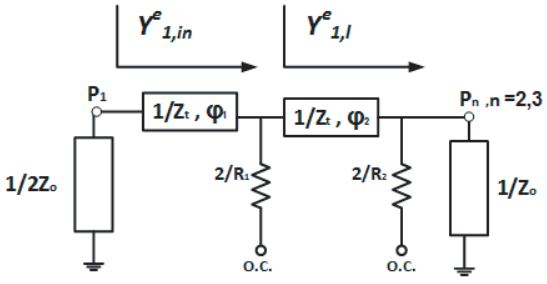

Figure 5. Even-mode bisection of the proposed PD in admittance representation, input admittance as seen at P_1.

3.1.1. Even-Mode Analysis at Port 1 (P1)

With even-mode excitation, an equal magnitude in phase signals is applied to output ports, i.e., $V_{g2} = V_{g3}$. Therefore, no voltage difference across the isolation resistors exists, and the circuit is bisected

with an open circuit (O.C.) i.e., isolation resistors have no effect in even mode analysis. Moreover, there is no current flowing through the short circuit between the inputs of the TLs at port 1; therefore, the impedance at port 1 is seen as $2Z_o$. Fig. 5 shows the even mode bisection where the voltage generators are omitted for simplicity. Since the design is based on insertion of parallel stub, it is convenient to use the admittance representation of TL. For perfect input and output matching:

$$S^e_{11} = S^e_{nn} = S^o_{nn} = 0, \quad n = 2, 3 \tag{1}$$

where S^e_{11} is the even-mode scattering parameter at Port 1 (P_1), S^e_{nn} the even-mode S-parameter at Port n (P_n), and S^o_{nn} the odd-mode S-parameter at P_n. Using Cohn's procedure for the two-section WPD, the input admittance at P_1, $Y^e_{1,in}$ is calculated as follows:

$$Y^e_{1,in} = \frac{1}{Z_t} \frac{Y^e_{1,l} + j\dfrac{\tan\varphi_1}{Z_t}}{\dfrac{1}{Z_t} + jY^e_{1,l}\tan\varphi_1} \tag{2}$$

$$Y^e_{1,l} = \frac{1}{Z_t} \frac{\dfrac{1}{Z_o} + j\dfrac{\tan\varphi_2}{Z_t}}{\dfrac{1}{Z_t} + j\dfrac{1}{Z_o}\tan\varphi_2} \tag{3}$$

The even-mode scattering parameter at P_1 is given by:

$$S^e_{11} = \frac{\dfrac{1}{2Z_o} - Y^e_{1,in}}{\dfrac{1}{2Z_o} + Y^e_{1,in}} \tag{4}$$

From Eq. (1) and Eq. (4) we get:

$$Y^e_{1,in} = \frac{1}{2Z_o} \tag{5}$$

Substituting Eq. (5) into Eq. (2) and rearranging, we have:

$$Z_t Y^e_{1,l} = \frac{j2Z_o\tan\varphi_1 - Z_t}{jZ_t\tan\varphi_1 - 2Z_o} \tag{6}$$

Then, rearrange Eq. (3), to obtain:

$$Z_t Y^e_{1,l} = \frac{Z_t + jZ_o\tan\varphi_2}{Z_o + jZ_t\tan\varphi_2} \tag{7}$$

Equate Eq. (6) and Eq. (7) to get:

$$jZ_t^2(\tan\varphi_1 + \tan\varphi_2) - Z_tZ_o[1 - \tan\varphi_1\tan\varphi_2] - j2Z_o^2(\tan\varphi_1 + \tan\varphi_2) = 0 \tag{8}$$

3.1.2. Even-Mode Analysis at Port n (Pn)

The input admittance at P_n, $Y^e_{n,in}$, as in Fig. 6, is calculated from:

$$Y^e_{n,in} = \frac{1}{Z_t} \frac{Y^e_{n,l} + j\dfrac{\tan\varphi_2}{Z_t}}{\dfrac{1}{Z_t} + jY^e_{n,l}\tan\varphi_2} \tag{9}$$

$$Y^e_{n,l} = \frac{1}{Z_t} \frac{\dfrac{1}{2Z_o} + j\dfrac{\tan\varphi_1}{Z_t}}{\dfrac{1}{Z_t} + j\dfrac{1}{2Z_o}\tan\varphi_1} \tag{10}$$

The even-mode scattering parameter at P_n is given by:

$$S^e_{nn} = \frac{\frac{1}{Z_o} - Y^e_{n,in}}{\frac{1}{Z_o} + Y^e_{n,in}} \tag{11}$$

Repeating the same steps carried out in Eqs. (5) to (7) to get the following equation:

$$jZ_t^2 (\tan\varphi_1 + \tan\varphi_2) - Z_t Z_o [\tan\varphi_1 \tan\varphi_2 - 1] - j2Z_o^2 (\tan\varphi_1 + \tan\varphi_2) = 0 \tag{12}$$

From Eqs. (8) and (12), we get:

$$Z_t = \sqrt{2} Z_o \tag{13}$$

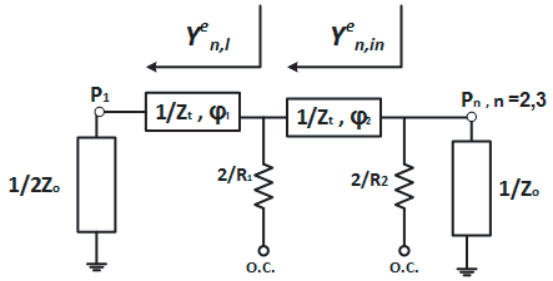

Figure 6. Even-mode bisection of the proposed PD in admittance representation, input admittance as seen at P_n.

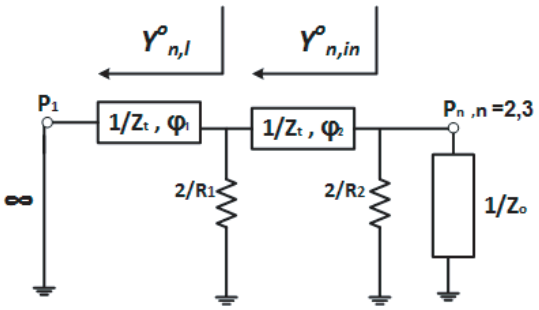

Figure 7. Odd-mode bisection of the proposed PD in admittance representation, input admittance as seen at P_n.

3.1.3. Odd-Mode Analysis at Port n (Pn)

With odd-mode excitation, an equal magnitude, out of phase signals are applied to output ports. Therefore, there is a voltage null along the mid-point of the circuit, and it is bisected by using ground as in Fig. 7. The input admittance at P_n, $Y^o_{n,in,}$ can be found from:

$$Y^o_{n,in} = \frac{2}{R_2} + \frac{1}{Z_t} \frac{Y^o_{n,l} + j\frac{\tan\varphi_2}{Z_t}}{\frac{1}{Z_t} + jY^o_{n,l}\tan\varphi_2} \tag{14}$$

$$Y^o_{n,l} = \frac{2}{R_1} - j\frac{1}{Z_t \tan\varphi_1} \tag{15}$$

The odd-mode scattering parameter at P_n is:

$$S^o_{nn} = \frac{\frac{1}{Z_o} - Y^o_{n,in}}{\frac{1}{Z_o} + Y^o_{n,in}} \tag{16}$$

From Eqs. (1) and (16), we have:

$$Y^o_{n,in} = \frac{1}{Z_o} \tag{17}$$

Substituting Eqs. (17) into (14) and rearranging, we get:

$$Z_t Y^o_{n,l} = \frac{jZ_o R_2 \tan\varphi_2 - Z_t R_2 + 2Z_o Z_t}{jZ_t R_2 \tan\varphi_2 - j2Z_o Z_t \tan\varphi_2 - Z_o R_2} \tag{18}$$

Also, rearranging Eq. (15), we get:

$$Z_t Y^o_{n,l} = \frac{2Z_t \tan\varphi_1 - jR_1}{R_1 \tan\varphi_1} \tag{19}$$

Equating Eqs. (18) and (19), we get:

$$jZ_oR_1R_2\tan\varphi_1\tan\varphi_2 - Z_tR_1\tan\varphi_1(R_2+2Z_o) = j2Z_t^2R_2\tan\varphi_1\tan\varphi_2 - j4Z_oZ_t^2\tan\varphi_1\tan\varphi_2$$
$$-2Z_oZ_tR_2\tan\varphi_1 + Z_tR_1R_2\tan\varphi_2 - 2Z_oZ_tR_1\tan\varphi_2 + jZ_oR_1R_2 \tag{20}$$

First, work with the real part of Eq. (20) to get a formula for the first isolation resistor R_1:

$$R_1 = \frac{2Z_oR_2\tan\varphi_1}{R_2(\tan\varphi_1+\tan\varphi_2) - 2Z_o(\tan\varphi_1+\tan\varphi_2)} \tag{21}$$

Second, work with the imaginary part to get a formula for the second isolation resistor R_2, where R_1 is substituted from Eq. (20) and Z_t substituted from Eq. (13):

$$R_2 = \frac{4Z_o\tan\varphi_2(\tan\varphi_1+\tan\varphi_2) + 2\sqrt{2}Z_o\sqrt{\tan\varphi_2(\tan\varphi_1+\tan\varphi_2)}\sqrt{\tan\varphi_1\tan\varphi_2-1}}{1+2\tan\varphi_2(\tan\varphi_1+\tan\varphi_2)-\tan\varphi_1\tan\varphi_2} \tag{22}$$

3.2. ABCD Matrix Analysis

In order to find the equivalency between the parameters of simplified structure $[(Z_t,\varphi_1),(Z_t,\varphi_2)]$ of Fig. 3 and the detailed one $[(Z_1,\theta_1,\theta_{11}$ and $Z_{s1},\theta_{s1}),(Z_1,\theta_2,\theta_{22}$ and $Z_{s2},\theta_{s2})]$ of Fig. 2, the ABCD matrix is used. Start with the first section as shown in Fig. 8 where the open shunt stub admittance Y_{s1} is represented as follows:

$$Y_{s1} = jB_1 = j\frac{\tan\theta_{s1}}{Z_{s1}} \tag{23}$$

where B_1 is the stub susceptance for the first section.

$$M_1M_2M_3 = \begin{bmatrix} \cos\varphi_1 & jZ_t\sin\varphi_1 \\ j\dfrac{\sin\varphi_1}{Z_t} & \cos\varphi_1 \end{bmatrix} = \begin{bmatrix} \cos\theta_1 & jZ_1\sin\theta_1 \\ j\dfrac{\sin\theta_1}{Z_1} & \cos\theta_1 \end{bmatrix} \begin{bmatrix} 1 & 0 \\ jB_1 & 1 \end{bmatrix} \begin{bmatrix} \cos\theta_{11} & jZ_1\sin\theta_{11} \\ j\dfrac{\sin\theta_{11}}{Z_1} & \cos\theta_{11} \end{bmatrix} \tag{24}$$

Multiplying the right hand matrices, equating element A of both matrices and solve for B_1:

$$B_1 = \frac{\cos(\theta_1+\theta_{11}) - \cos\varphi_1}{Z_1\sin\theta_1\cos\theta_{11}} \tag{25}$$

Similarly, equate element C of both matrices and solve for Z_1:

$$Z_1 = Z_t\frac{\cos\theta_{11} - \cos\varphi_1\cos\theta_1}{\sin\varphi_1\sin\theta_1}, \quad Z_t = \sqrt{2}Z_o \tag{26}$$

From Eqs. (23) and (25) and arranging, we get that

$$Z_{s1} = \tan\theta_{s1}\frac{Z_1\sin\theta_1\cos\theta_{11}}{\cos(\theta_1+\theta_{11}) - \cos\varphi_1} \tag{27}$$

Repeating the ABCD matrix procedure for the second section of Fig. 9 where the open shunt stub admittance Y_{s2} is represented as follows:

$$Y_{s2} = jB_2 = j\frac{\tan\theta_{s2}}{Z_{s2}} \tag{28}$$

where B_2 is the stub susceptance for the second section

$$Z_{s2} = \tan\theta_{s2}\frac{Z_1\sin\theta_2\cos\theta_{22}}{\cos(\theta_2+\theta_{22}) - \cos\varphi_2} \tag{29}$$

A UWB 2-way two-section WPD of unequal electrical lengths can be designed by substituting in Eqs. (13), (21), (22) for the desired φ_1/φ_2 ratio and in order to determine the Tee-sections parameters, substituting in Eqs. (26), (27), (29). The only remaining step is to determine the ratio between the electrical lengths of sections one and two, i.e., φ_1/φ_2, which will be investigated in the following section.

4. PARAMETRIC ANALYSIS OF Φ_1 AND Φ_2

In this section, a parametric analysis of φ_1 and φ_2 is introduced to determine the electrical length ratio (φ_1/φ_2) that meets the required performance parameters such as input return loss, output return loss, insertion loss, isolation and fractional bandwidth. This is achieved by simulating the simplified structure for different φ_1/φ_2 ratios as follows:

1. Calculate R_1 and R_2 using Eqs. (21) and (22) for different φ_1/φ_2.
2. Carry out the simulation as in Fig. 3 for each φ_1/φ_2 to get the performance parameters such as isolation, input return loss, output return loss, insertion loss and fractional bandwidth (FBW).
3. Plot performance parameters versus φ_1/φ_2 ratio. For example, the isolation (S_{32}) for various φ_1/φ_2 ratios is shown Fig. 10 where S_{32} has lower variation for $\varphi_1/\varphi_2 = 1/2$ and 2 for a wide range of frequency, and it is better than -10 dB.

Figure 11 shows different performance parameters versus φ_1/φ_2 (Note that the input return loss and exceeded insertion loss are excluded from the graph, as they are constant for different φ_1/φ_2). From Fig. 11, $\varphi_1/\varphi_2 = 1/2$ and 2 achieve better performance than other ratios. Here in this proposed work, $\varphi_1/\varphi_2 = 2$ is chosen as it gives better flexibility in the implementation process.

5. DESIGN AND IMPLEMENTATION OF UWB 2-WAY PD

It is desired to design a 2-way PD with the following specifications: $S_{11} \leq -10$ dB, $|S_{21}| = 3$ dB + 1.0, $S_{22} = S_{33} \leq -10$ dB and $S_{32} = S_{32} \leq -10$ dB. A schematic diagram of the proposed UWB modified Wilkinson power divider ($N = 2$) is shown in Fig. 2.

5.1. 2-Way Power Divider Initial Design Procedure

In the previous section, a detailed analytical solution for the proposed two-section unequal electrical length power divider is introduced. This analytical solution is used in this section to get an initial numerical solution for the proposed power divider according to the following procedure:

1. Determine the characteristic impedance of each section ($Z_{t1} = Z_{t2} = Z_t$): From Eq. (13), for input and output ports matched at $Z_o = 50\ \Omega$, then $Z_t = \sqrt{2}Z_o = 70.71\,\Omega$.
2. Determine the electrical length of each section (φ_1, φ_2): for two-section conventional WPD, the total electrical length $\varphi_t = \varphi_1 + \varphi_2 = \pi$. For this proposed method, $\varphi_1 = 2\varphi_2$, then $\varphi_1 = 120°$, and $\varphi_2 = 60°$.
3. Calculate the isolation resistors (R_1, R_2) using Eqs. (21) and (22), then $R_1 \approx 122\ \Omega$ and $R_2 \approx 169\ \Omega$.
4. Determine the physical design parameters of the 1st section: The primary TL has an electrical length, θ_1, of quarter wavelength leaving $\lambda/12$ electrical length divided equally between θ_{11}, θ_{s1}, i.e., $\theta_1 = 90°$, $\theta_{11} = 15°$ and $\theta_{s1} = 15°$. Using Eq. (26), the characteristic impedance of the main TL, $Z_1 = 78.87\,\Omega$. From Eq. (27), the stub characteristic impedance, $Z_{s1} = 84.63\,\Omega$.
5. Determine the physical design parameters of the 2nd section: For $\theta_2 = 30°$, $\theta_{22} = 15°$ and $\theta_{s2} = 15°$. Using Eq. (29), the stub characteristic impedance, $Z_{s2} = 58\,\Omega$. The calculated parameters of the divider's ideal TL representation are summarized in Table 1.

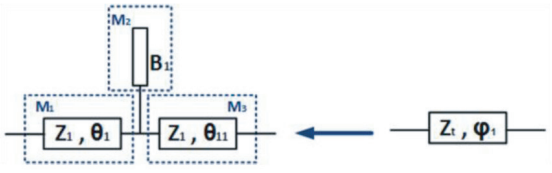

Figure 8. Matrices identification of the first section.

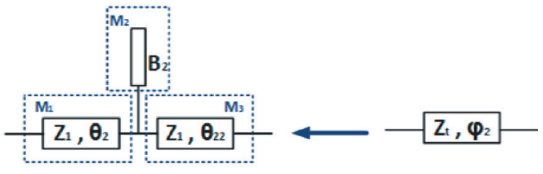

Figure 9. Matrices identification of the second section.

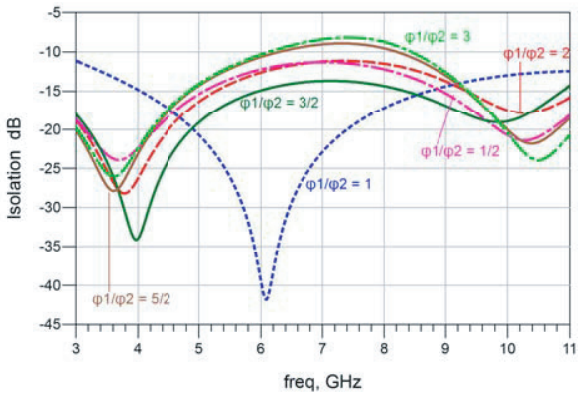

Figure 10. Isolation for simplified two-section WPD for different φ_1/φ_2 ratios.

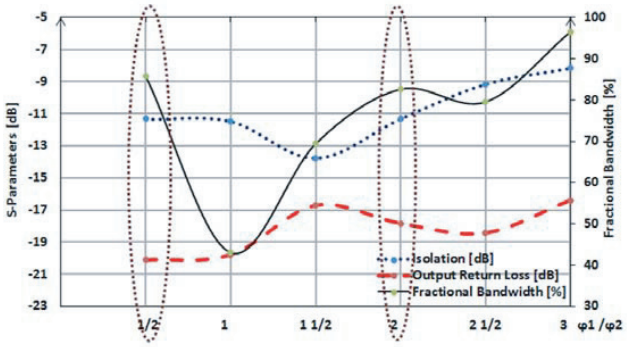

Figure 11. φ_1/φ_2 versus Isolation, Output return loss and Fractional bandwidth.

Table 1. Calculated initial parameters for the proposed ideal TL 2-way PD.

Input and output ports						Z_o	θ_o			
						50 Ω	50°/130°			
1st Section						2nd Section				
Z_1	θ_1	θ_{11}	Z_{s1}	θ_{s1}	R_1	θ_2	θ_{22}	Z_{s2}	θ_{s2}	R_2
78.8	90	15	84.6	15	122	30	15	58	15	169

5.2. Proposed 2-Way Power Divider Circuit Simulation

To examine the performance of the proposed UWB modified WPD, the initial design parameters calculated in the previous section are modeled as an ideal TL circuit. The Advanced Design System from Agilent (now known as Keysight) simulation package is used in this work. The simulated S-parameters for the proposed TL PD are shown in Fig. 12, where it can be noticed that this design fulfils the desired requirements even without the need for any further tuning or optimization.

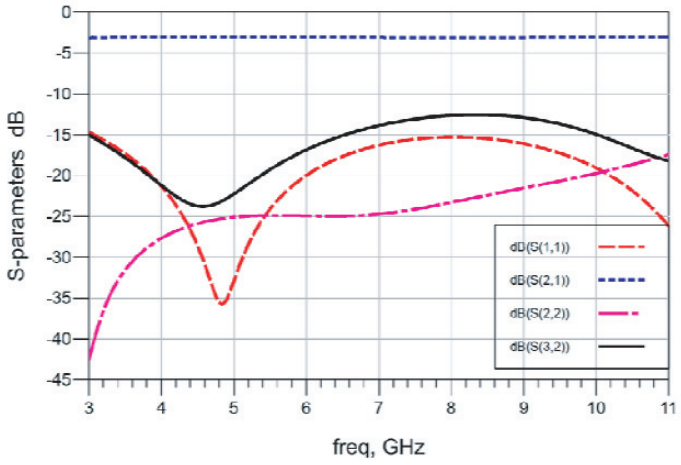

Figure 12. S-parameters for the proposed TL form of the divider according to initial calculation.

5.3. Implementation of the Proposed 2-Way Power Divider

The proposed UWB 2-way PD realized using a commercial Rogers RT/duroid 5880 substrate with height $h = 0.787$ mm, dielectric constant $\varepsilon_r = 2.2$, and loss tangent $\tan\delta = 0.0009$. The proposed TL PD is converted to microstrip (MS) at the center frequency 6.85 GHz ($f_c = \frac{f_l+f_u}{2} = \frac{3.1+10.6}{2} = 6.85$ GHz) where, the physical dimensions obtained are tabulated in Table 2. A schematic diagram of the 2-way PD in microstrip is shown in Fig. 13, where no tees or corners are added, and since the Duroid 5880 has a low dissipation factor, it is predicted that the ideal TL form and MS form without discontinuities will give almost identical S-parameter performance. This is validated through circuit simulation as shown in Fig. 14.

Table 2. Physical dimensions of the proposed initial 2-way PD.

Input/output (mm)					w_o		L_o	
					2.41		4.42/11.42	
1st Section (mm)					2nd Section (mm)			
w_1	L_1	L_{11}	w_{s1}	L_{s1}	L_2	L_{22}	w_{s2}	L_{s2}
1.1	8.15	1.36	0.97	1.36	2.72	1.2	1.8	1.55

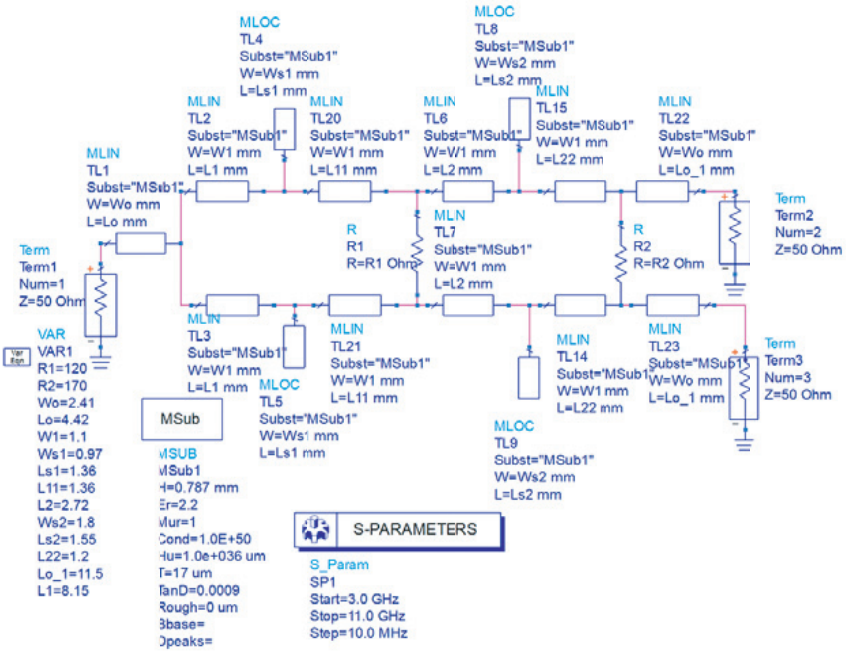

Figure 13. Microstrip form of the proposed 2-way PD without discontinuities.

In order to get a practical layout that can be fabricated, tees and corners must be added as in Fig. 15, where lengths, such as L_1, L_{11}, L_2, and L_{22}, are divided into sub-lengths. Despite taking tees and corners lengths in calculations, it still causes the performance to degrade as in Fig. 16.

To enhance the performance, a tuning analysis for design parameters is carried out to get the final physical dimensions of the 2-way PD as listed in Table 3. The generated layout is simulated using EM simulator. An "EM-Circuit Co-Simulation" is carried out, where the generated EM model for the proposed divider has been placed back in the schematic. Then, the ideal isolation resistors are added, and the whole design is simulated. To get practical performance, the isolation resistors are replaced by their S-parameter models. From the simulation, it is noticed that the resistor model gives a slight deviation in S-parameter, i.e., the design is less sensitive to resistor models. The proposed 2-way PD is fabricated

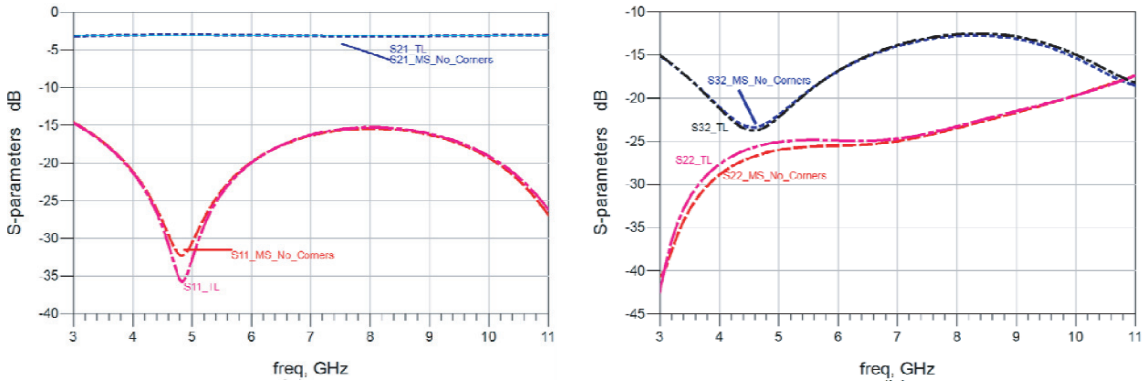

(a) (b)

Figure 14. Performance of the TL 2-way PD versus Microstrip without discontinuities, (a) insertion loss and input return loss, and (b) output return loss and isolation.

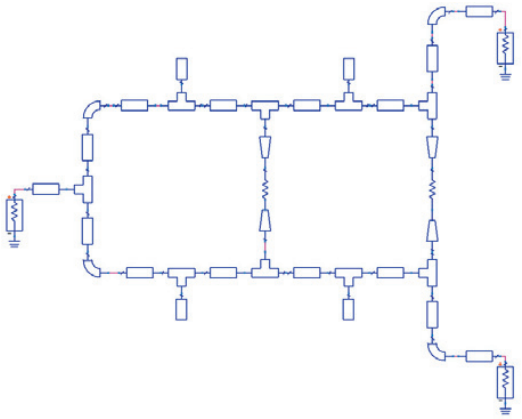

Figure 15. Microstrip form of the proposed 2-way PD with tees and corners.

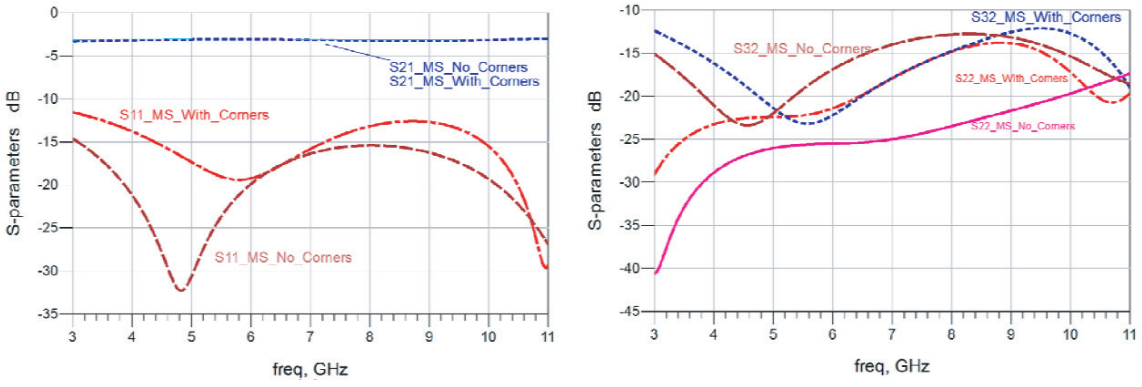

(a) (b)

Figure 16. Performance of the TL 2-way PD versus MS with discontinuities, (a) insertion loss, input return loss, and (b) output return loss, isolation.

as shown in Fig. 17. *S*-parameters measurements are carried out using Rohde & Schwarz ZVB20 vector 4-port network analyzer. Table 4 presents the simulated and measured *S*-parameters of the proposed 2-way PD, where the measured input return loss is better than 10 dB; measured insertion loss is 3+0.9 dB; measured output return loss is better than 14.5 dB; measured isolation is better than 13.56 dB for the

Table 3. Final dimensions for the proposed microstrip 2-way PD on Duroid 5880.

Input/output (mm)					W_o		L_o	
					2.41		4.42/11.42	
1st Section (mm)					2nd Section (mm)			
W_1	L_1	L_{11}	W_{s1}	L_{s1}	L_2	L_{22}	W_{s2}	L_{s2}
1	7.72	1.22	0.97	1.27	2.72	1.2	1.5	1.55
Isolation Resistors (Ω)					R_1		R_2	
					120		180	

Table 4. EM-circuit co-simulated and measured S-parameters of the proposed 2-way PD.

	$S_{11\,\mathrm{dB}}$	$\lvert S_{21}\rvert_{\mathrm{dB}}$	$S_{22\,\mathrm{dB}}$	$S_{32\,\mathrm{dB}}$
Requirements	≤ -10	$3 + 1.0$	≤ -10	≤ -10
EM-Circuit Co-Simulation	≤ -11.54	$3 + 0.25$	≤ -16.26	≤ -13.58
Measurements	≤ -10.07	$3 + 0.9$	≤ -14.5	≤ -13.56

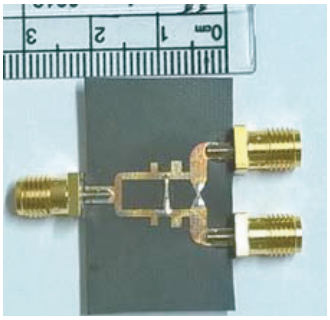

Figure 17. Fabricated 2-way power divider.

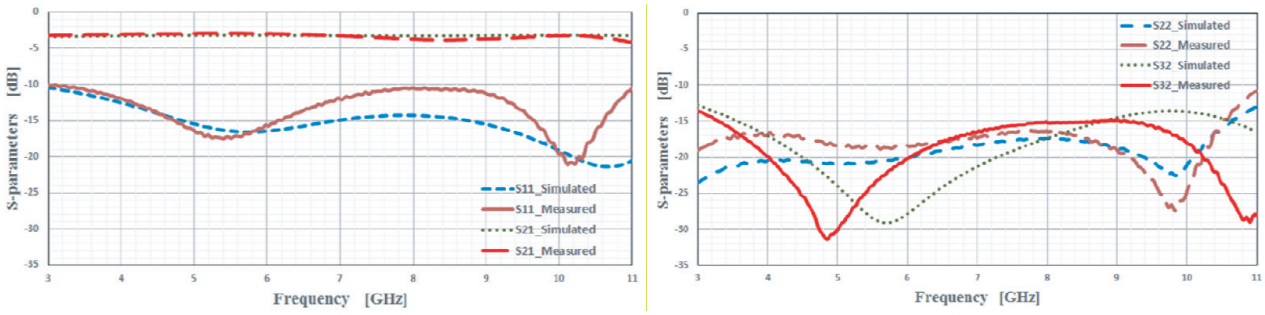

(a) (b)

Figure 18. Measurements versus EM-circuit co-simulated results of 2-Way PD, (a) input return loss, insertion loss, (b) output return loss and isolation.

entire UWB range. Fig. 18 shows the measurements versus the EM-Circuit Co-Simulation results for the proposed 2-way power divider. Although all required specifications are satisfactorilly achieved, some discrepancies between measured and simulated results are noticed especially in S_{32}. This deviation may be due to fabrication tolerances, isolation resistors soldering, and parasitics. Otherwise, measurements agree well with simulations, which verifies the design equations as well as the proposed methodology.

5.4. Comparison to Other Published Work

Table 5 shows a comparative study for this work with other published UWB MS power dividers that use stubs and have similar substrate parameters. Ref. [19] introduced a single section WPS with single stub-matching network. Although our proposed PD has two sections, it occupies less area with improved insertion loss, output return loss and port isolation compared with that of [19]. Ref. [11] introduced a single section WPD with delta stub and single isolation resistor. Our proposed PD achieves comparable performance with improved isolation. Ref. [12] shows single section unequal WPD with two folded shunt $\lambda/4$ short circuit stubs and single isolation resistor. Despite the complexity of the design, it achieves moderate performance with large area. The proposed work enhancement percentage over [13] is presented.

The enhancement percentage of the proposed work over [13] is presented as both works use two-section WPD with total number of two resistors. Despite the fact that [13] has a complicated structure of using three open stubs and two aperture backed inter digital-coupled lines, and has Defected Ground Structure (DGS), our proposed 2-way PD achieves 50% area reduction without any DGS or other reduction techniques. In addition, this novel technique without intensive CAD optimization improves output matching, isolation and insertion loss by 45%, 23% and 13%, respectively. Meanwhile, it achieves comparable input return loss to others. The exceeded insertion loss is less than 0.9 and can be enhanced by using fabrication facility with better tolerances and modeling the soldering points properly.

Table 5. A comparative study for this proposed 2-way PD with other published 2-way PD.

Specs.	[19]	[11]	[12]	[13]	This Work	Enhancement % over [13]
Freq. GHz	3.1–10.6	3.1–10.6	2.9–10.9	3.1–10.6	3.1–10.6	-
$S_{11\,dB}$	≈ -11	-10	≈ -8.5	-10	-10	-
$S_{21\,dB}$	-3-2	-3–0.3	≈ -3–1	≈ -3–1.5	-3–0.9	$\approx 13\%$
$S_{22\,dB}$	-10	-15	≈ -6	-10	-14.5	$\approx 45\%$
$S_{23\,dB}$	-5	-10	-10	-11	-13.56	$\approx 23\%$
$Area^2_{mm}$	$22 * 20$	$18 * 13$	$34 * 24$	$20 * 45$	$22 * 15$	$\approx 50\%$
substrate ε_r and h in mm	2.2, 0.787	3.38, 0.508	2.2, 1.0	2.2, 0.787	2.2, 0.787	-

6. CONCLUSION

In this paper, a novel 2-way power divider for UWB systems is proposed. The proposed 2-way power divider has two sections of unequal electrical lengths from modified Wilkinson power divider. The modification in WPD is by inserting a stub matching network on each section to improve matching and broaden the bandwidth. A detailed analytical solution for the proposed 2-way power divider is discussed to obtain exact-closed form design equations. The analytical solution is based on the "even-odd mode" method. Moreover, the stub susceptance equations are obtained using the "ABCD matrix" approach. In order to decide the ratio between the electrical lengths of the two sections, a parametric analysis is carried out. The proposed 2-way power divider's design methodology is employed to utilize 2-way power divider for UWB systems. The initial TL 2-way PD based on the analytical solution verifies the requirements without the need for further optimization. The proposed 2-way PD is fabricated and measured. Good agreement between simulated and measured results is achieved which verifies the design equations and methodology. The comparison between the fabricated 2-way PD and similar microstrip PDs shows improvement of 13% insertion loss, 45% output return loss and 23% isolation with 50% area reduction without any intensive optimization.

REFERENCES

1. Wilkinson, E. J., "An n-way hybrid power divider," *IEEE Transactions on Microwave Theory and Techniques*, Vol. 8, No. 1, 116–118, Jan. 1960.
2. Cohn, S. B., "A class of broadband three-port TEM-mode hybrids," *IEEE Transactions on Microwave Theory and Techniques*, Vol. 16, No. 2, 110–116, Feb. 1968.
3. El-Tager, A. M. E., A. M. A. H. El-Akhdar, and H. M. S. El-Henawy, "Analysis of coupled microstrip lines for quad-band equal power dividers/combiners," *Progress In Electromagnetics Research B*, Vol. 41, 187–211, 2012.
4. Kim, T., B. Lee, and M.-J. Park, "Dual-band unequal Wilkinson power divider with reduced length," *Microwave and Optical Technology Letters*, Vol. 52, No. 5, 1187–1190, May 2010.
5. Chi, P. and K. Ho, "Design of dual-band coupler with arbitrary power division ratios and phase differences," *IEEE Transactions on Microwave Theory and Techniques*, Vol. 62, No. 12, 2965–2974, Oct. 2014.
6. Kasim, F. R. H., M. A. S. Alkanhal, and A.-F. A. Sheta, "UWB Wilkinson power divider using tapered transmission lines," *PIERS Proceedings*, 882–884, Moscow, Russia, Aug. 19–23, 2012.
7. Mencia-Oliva, B., A. M. Pelaez-Perez, P. Almorox-Gonzalez, and J. I. Alonso, "New technique for the design of ultra-broadband power dividers based on tapered lines," *2009 IEEE MTT-S International Microwave Symposium Digest*, 493-496, Boston, MA, Jun. 2009.
8. Chiang, C. T. and B.-K. Chung, "Ultra wideband power divider using tapered line," *Progress In Electromagnetics Research*, Vol. 106, 61–73, 2010.
9. Chang, L., C. Liao, L.-L. Chen, W. Lin, X. Zheng, and Y.-L. Wu, "Design of an ultra-wideband power divider via the Coarse-Grained parallel Micro-Genetic algorithm," *Progress In Electromagnetics Research*, Vol. 124, 425–440, 2012.
10. Ahmed, O. and A. R. Sebak, "A modified Wilkinson power divider/combiner for ultrawideband communications," *2009 IEEE Antennas and Propagation Society International Symposium*, 1-4, Charleston, SC, Jun. 2009.
11. Zhou, B., H. Wang, and W.-X. Sheng, "A modified UWB Wilkinson power divider using delta stub," *Progress In Electromagnetics Research Letters*, Vol. 19, 49–55, 2010.
12. Wei, F., X. W. Shi, P. Y. Qin, and Y. J. Guo, "Compact UWB power divider with unequal distribution ratio," *2014 International Workshop on Antenna Technology: Small Antennas, Novel EM Structures and Materials, and Applications (iWAT)*, 297–299, Sydney, NSW, Mar. 2014.
13. Liu, W.-Q., F. Wei, C.-H. Pang, and X.-W. Shi, "Design of a compact ultra-wideband power divider," *2012 International Conference on Microwave and Millimeter Wave Technology (ICMMT)*, Vol. 2, 1–3, Shenzhen, May 2012.
14. Abbosh, A., "Design of ultra-wideband three-way arbitrary power dividers," *IEEE Transactions on Microwave Theory and Techniques*, Vol. 56, No. 1, 194–201, Jan. 2008.
15. Guo, L., A. Abbosh, and H. Zhu, "Ultra-wideband in-phase power divider using stepped-impedance three-line coupled structure and microstrip-to-slotline transitions," *Electronics Letters*, Vol. 50, No. 5, 383–384, Feb. 2014.
16. Song, K., Y. Zhu, Q.Duan, M. Fan, and Y. Fan, "Extremely compact ultra-wideband power divider using hybrid slotline/microstrip-line transition," *Electronics Letters*, Vol. 51, No. 24, 2014–2015, Nov. 2015.
17. Oraizi, H. and A.-R. Sharifi, "Design and optimization of broadband asymmetrical multisection Wilkinson power divider," *IEEE Trans. Microwave Theory and Techniques*, Vol. 54, No. 5, 2220–2231, May 2006.
18. Shamaileh, K. A., M. Almalkawi, V. K. Devabhaktuni1, N. I. Dib, B. Henin, and A. Abbosh, "Non-uniform transmission line ultra-wideband Wilkinson power divider," *Progress In Electromagnetics Research C*, Vol. 44, 1–11, 2013.
19. Ahmed, O. M. H. and A. R. Sebak, "Experimental investigation of new ultra wideband in-phase and quadrature-phase power splitters," *Journal of Electromagnetic Waves and Applications*, Vol. 23, Nos. 17–18, 2261–2270, Apr. 2012.